PHYSICAL REVIEW A **87**, 060501(R) (2013)

Resonant coherent excitation of the lithiumlike uranium ion: A scheme for heavy-ion spectroscopy

Y. Nakano,[1,2,*] Y. Takano,[1,3] T. Ikeda,[1] Y. Kanai,[1] S. Suda,[1,2] T. Azuma,[1,2] H. Bräuning,[4] A. Bräuning-Demian,[4] D. Dauvergne,[5] Th. Stöhlker,[4,6,7] and Y. Yamazaki[1,3]

[1]*RIKEN Advanced Science Institute, Saitama 351-0198, Japan*

[2]*Department of Physics, Tokyo Metropolitan University, Tokyo 192-0397, Japan*

[3]*Graduate School of Arts and Sciences, University of Tokyo, Tokyo 153-8902, Japan*

[4]*GSI Helmholtzzentrum für Schwerionenforschung, D-64291 Darmstadt, Germany*

[5]*IPNL, Université de Lyon, Université Claude Bernard Lyon I, CNRS/IN2P3, F-69622 Villeurbanne, France*

[6]*Helmholtz-Institut Jena, D-07743 Jena, Germany*

[7]*Institut für Optik und Quantenelektronik, Friedrich-Schiller-Universität, D-07743 Jena, Germany*

(Received 7 September 2012; published 7 June 2013)

We report our observation of the resonant fluorescence from highly charged uranium ions. Using the resonant coherent excitation (RCE) technique, the $2s$-$2p_{3/2}$ transition in 191.68 MeV/u Li-like U^{89+} ions was excited at 4.5 keV with a resonance width of 4.4 eV. The result demonstrated that the RCE can be applied to resonant fluorescence spectroscopy of high-Z ions up to uranium with high efficiency and resolution.

DOI: 10.1103/PhysRevA.87.060501 PACS number(s): 32.30.−r, 34.50.Fa, 61.85.+p

High-precision spectroscopy of simple atomic systems is one of the most fundamental and critical interests in natural science, having revealed a number of new phenomena understood in our modern quantum physics. Advances in high-resolution tunable lasers are dramatically improving the accuracy of resonant fluorescence spectroscopy techniques that enable testing of rigorous theories and increase the accuracy of fundamental constants [1]. However, such laser technologies are not applicable in the x-ray domain, although the x-ray spectroscopy with high-Z ions uniquely provides the opportunity to prove the effects of relativity, higher-order quantum electrodynamics (QED), and the structure of nuclei. So far the spectroscopic study of high-Z few-electron ions is only available by measuring the energy of x rays emitted after collisional excitation [2], radiative electron capture [3], etc., using semiconductor detectors or spectrometers. Therefore the quality of x-ray spectroscopy is experimentally limited by the detector resolution and efficiency to a point inferior to that achieved by laser fluorescence methods. Innovations in high-resolution tunable light sources in the short-wavelength region would offer unique opportunities to explore atomic and nuclear structures with an unprecedented precision, enabling highly sensitive testing of rigorous theories. Indeed, for example, the recent advent of x-ray free-electron lasers has demonstrated the potential for the accurate determination of a higher-order QED effect by laser spectroscopy in the soft x-ray domain up to 200 eV [4].

Here we demonstrate a promising scheme for resonant fluorescence spectroscopy in the x-ray domain using resonant coherent excitation (RCE). The RCE refers to the electronic excitation of the fast ions penetrating through a monocrystalline target. In the reference frame of the fast ions, the periodic Coulomb potential in the crystal appears as an electromagnetic field oscillating in the x-ray frequency domain [5]. When the oscillation frequency coincides with the absorption frequency of the ions in their rest frame, they can be resonantly excited. Because this frequency can be controlled by changing the relative angle between the ion velocity and crystallographic orientation, resonant fluorescence spectroscopy is performed by observing the x-ray fluorescence as a function of the incident angle.

Several transitions in simple atomic systems accessible by the RCE process are shown in Fig. 1, along with currently available experimental data [6–13]. The increase in ion-beam energy has enabled higher excitation energies of the RCE process covering the $1s$-$2p$ transition of H-like ions in the range of nuclear charge numbers $Z = 5$–26, i.e., transition energies from 200 eV to 7 keV. Recent experimental studies using high-energy beams at the Heavy Ion Medical Accelerator in Chiba (HIMAC) have paved the way for various new schemes of coherent population control techniques in the x-ray domain [14–16]. In the near future, extremely high-energy ions up to 33 GeV/u will be provided by the Facility for Antiproton and Ion Research (FAIR) [17]. In principle, this allows the RCE process to cover transition energies up to the $1s$-$2p$ transition of H-like uranium at ∼100 keV. However, whether the RCE process can be exploited for heavier species ($Z \gg 26$) has remained a nontrivial open question. Experimental data about the coherence length of such high-Z ions in a solid target is lacking, for which a theoretical calculation is also difficult to obtain without experimental data [18]. In addition, electronic stopping and straggling increase with Z^2, causing significant broadening in the resonance spectrum. On the other hand, if RCE of a high-Z ion can be demonstrated, it could be applied as a universal technique to study a broad range of ions covering the x- and gamma-ray regime. Furthermore, the spectroscopy with RCE has the significant advantage of enabling to examine small amounts of in-flight particles obtained from high-energy accelerators without trapping them into a confined region. Therefore, a broad range of radioactive species from high-energy accelerators would also become available for analysis. In the present Rapid Communication, we aim to experimentally explore the feasibility of applying the RCE process to heavy species as a scheme for high-resolution spectroscopy in the x-ray domain.

To this end, we demonstrate our observation of the RCE process using the heaviest natural element, uranium ($Z = 92$).

*nakano-y@riken.jp

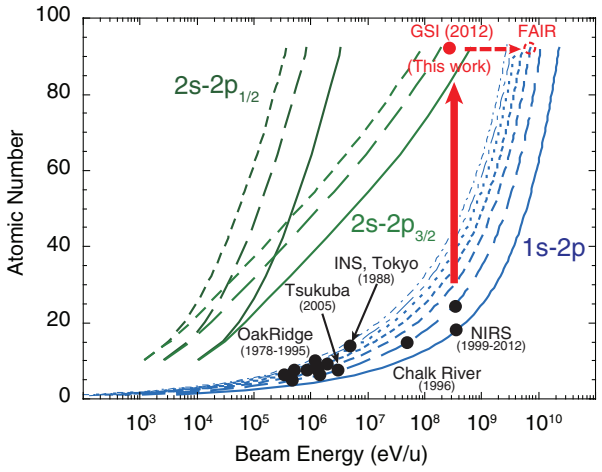

FIG. 1. (Color) Relationship between beam energy and atomic number required to observe the RCE process. The lines are calculated for the $1s$-$2p$ transition in H-like ions, and the $2s$-$2p_{1/2}$ and $2s$-$2p_{3/2}$ transitions in Li-like ions. The dots show experimental data reported to date.

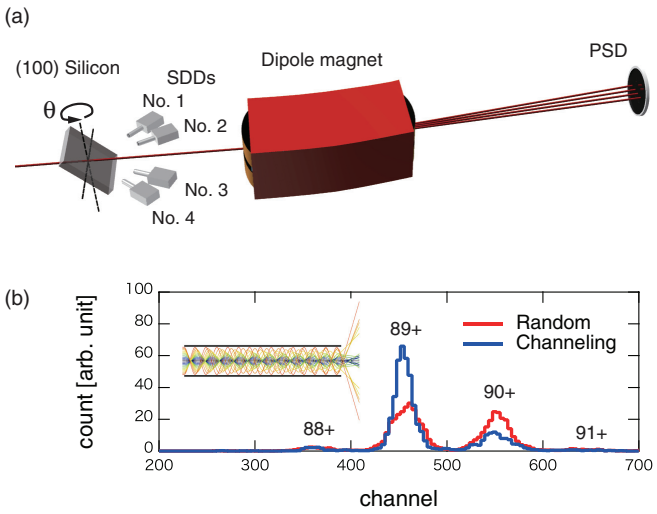

FIG. 2. (Color) (a) Schematic layout of the experimental setup. (b) The charge state distribution of the beam exiting the target crystal under random and (220) channeling conditions. The inset shows the (220) channeling trajectory simulation for the 193 MeV/u U^{89+} ions in a 10-μm-thick Si crystal.

We focused on the RCE of the $1s^2 2s$ - $1s^2 2p_{3/2}$ intrashell transition in Li-like U^{89+} ions with a 7-μm-thick (100) silicon crystal. We chose (220) planar channeling for the incidence condition, because the channeled U^{89+} ions are expected to avoid close collisions with target atoms [19–21]. The corresponding transition energy was reported as $\Delta E = 4459.37 \pm 0.21$ eV from an experimental study using a crystal spectrometer [22,23]. Under (220) planar channeling conditions, the ions pass through a periodic array of atomic strings on the atomic plane at frequency $\nu_{k,l}(\theta)$ given by

$$\nu_{k,l}(\theta) = \frac{\gamma v}{a}(\sqrt{2}k\cos\theta + l\sin\theta), \qquad (1)$$

where γv is the ion velocity multiplied by the relativistic Lorentz factor, a is the lattice constant of the Si crystal, and (k,l) is the two-dimensional Miller index specifying the set of atomic strings [24]. Angle θ represents the ion incident angle relative to the [110] axis, which satisfies the resonance condition of the RCE process when $h\nu_{k,l}(\theta)$ is equal to ΔE.

Experiments were conducted at GSI Helmholtzzentrum für Schwerionenforschung using the heavy-ion synchrotron (SIS). A high-precision goniometer developed at RIKEN [25] was installed in the target vacuum chamber in the Cave A experimental hall. Using an in-vacuum glass plate encoder, the angular resolution of the goniometer was less than 1 μrad. Thus, the systematic resolution of our instrument for the frequency $h\nu_{k,l}(\theta)$ is better than 0.001 eV, i.e., 0.2 ppm of the transition energy. We stored and accelerated U^{73+} ions in the SIS to a final beam energy of 193 MeV/u. The latter has been deduced from the circulation frequency at extraction. The extracted beam penetrated a stripping foil of 10.8 mg/cm^2 Al, in which the exit energy was calculated to be 191.68 MeV/u. The Li-like U^{89+} ions produced in the Al foil were transported to the target chamber through a pair of four-jaw slits placed at 6 m from each other, limiting the angular divergence to below 0.32 mrad. The schematic layout of the setup is shown in Fig. 2(a). To obtain the (220) plane horizontal, the target crystal was vertically tilted at 45° to the beam, which makes the pass length in the crystal equal to 10 μm. For the detection of deexcitation x rays, we installed four Peltier-cooled silicon drift detectors (SDDs) into the target chamber. SDDs No. 1 and No. 4 were installed at ±43°, and at a distance of 177.8 mm from the target within the same horizontal plane. For SDDs No. 2 and No. 3, the detection angle and distance were ±33° and 201.5 mm, respectively. Each detector has a large detection area of 80 mm^2 with an energy resolution of 180 eV at 5.9 keV [26]. Downstream of the crystal, the primary ion beam was charge separated by a dipole magnet and detected by a two-dimensional (2D) position-sensitive detector (PSD). The charge state distributions of the ions exiting the target crystal under random incidence and (220) channeling conditions are shown in Fig. 2(b). The fraction of U^{89+} was 55% under the random incidence condition, which is reproduced well by calculations based on the GLOBAL code [27]. When the ions were incident under (220) channeling conditions, the U^{89+} fraction increased up to 76% owing to the suppression of close collisions with target atoms. Additionally, the channeled beam was decreased in size and was slightly shifted to the higher-energy side (left-hand side) on the PSD. These reflect the suppression of large-angle scattering and energy loss of channeled ions in the target, respectively.

The RCE measurement was performed by observing the x-ray energy spectra under (220) planar channeling conditions at different θ. Figure 3(a) shows the contour plot of the raw x-ray energy spectra from SDD No. 3 observed by scanning θ at steps of 0.02°. X-ray spectra were measured at each angle for 3.5×10^5 ions counted at the PSD. With an average beam intensity of 2000 counts/s, the accumulation time was ~3 min/point. We observed two different x-ray lines corresponding to the $K\alpha$ of the Si target (1740 eV) and the deexcitation of the $2p_{3/2}$ state from the projectile U^{89+} ions (4459 eV). Note that the relativistic Doppler effect boosted the projectile's x-ray energy in the laboratory frame. In the

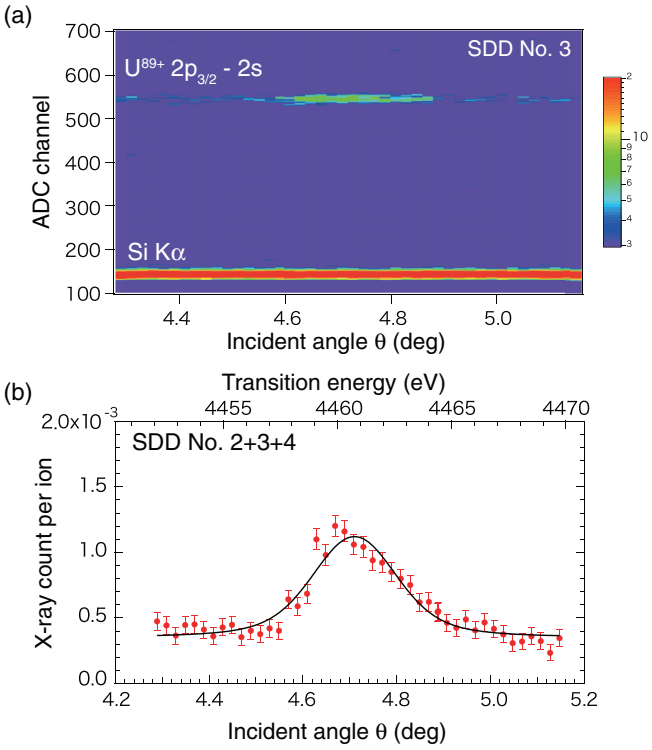

FIG. 3. (Color) (a) X-ray energy spectra observed with SDD No. 3 for different θ. (b) The total number of x rays observed with SDDs No. 2, No. 3, and No. 4 as a function of θ. The solid line is a Gaussian curve fitted to the data.

case of SDD No. 3, the Doppler factor was 1.56. In this 2D plot, a clear enhancement of the projectile x-ray intensity can be seen around the angle for the $(k,l) = (2,1)$ resonance, i.e., $\theta = 4.7^\circ$, whereas the one of the target radiation remains constant. This proves that the RCE process of the $2s$ -$2p_{3/2}$ transition in Li-like U^{89+} ions was successfully demonstrated. The projectile x-ray yields from SDDs No. 2, No. 3, and No. 4 are summed and plotted in Fig. 3(b) as a function of θ (lower axis) and corresponding transition energy (upper axis). The transition energy was obtained from Eq. (1) with an estimated mean beam energy in the target. In this procedure, we estimated the energy loss of the channeling ions to be 50% that of the random incident ions [28], which was calculated to be 0.29 MeV/u using the ATIMA code [29]. The consistency of the above assumption was confirmed from the difference in the beam position at the PSD under the channeling and random incident conditions [Fig. 2(b)]. The data from SDD No. 1 was not included in this analysis, due to the high background rate. The total x-ray yield shown in Fig. 3(b) formed a peak centered at the resonance angle, where the fluorescence rate was enhanced by a factor of 3 relative to that under the nonresonant condition. After the subtraction of nonresonant background x-ray emission and normalization by the charge fraction of U^{89+} (76%), the total resonance fluorescence yield observed by the three detectors was 9.6×10^{-4} counts/ U^{89+} ion. Because the beam intensity was 2×10^3 counts/s, the count rate of x-ray fluorescence during the measurement was more than 1 count/s using the three detectors. This owes to the large detection area of the detectors as well as the high excitation efficiency of the RCE method. From the geometrical detection efficiency of 1.2×10^{-3}, which is the sum of relativistic solid angles for the three detectors, the excitation efficiency of U^{89+} ions in the Si crystal was found be as high as 80%. In this estimation, we assumed an isotropic emission of decay radiation. In fact, no significant anisotropies were observed between the detectors at different angles, which is due to the averaging of alignment parameters over the different channeling trajectories.

TABLE I. Estimates of the contributions to the resonance width.

Factor	Value	Width (eV)
Longitudinal momentum spread	7×10^{-4}	3.1
Spread due to energy loss	0.15 MeV/u	1.9
Energy straggling	0.004 MeV/u	0.03
Angular divergence	0.32 mrad	0.37
Angular straggling	0.08 mrad	0.09

The solid line in the figure shows a Voigt curve fitted to the experimental data. The fitting showed the full width at half maximum (FWHM) to be 4.4 eV, and the peak transition energy to be $4460.9 \pm 0.1_{\text{stat.}} \pm 2.2_{\text{sys.}}$ eV, which agrees with the reported value [22,23]. Although the uncertainty of the beam energy from the SIS caused a large systematic error in the transition energy, the energy resolution of the present experiment is comparable to those of state-of-the-art crystal spectrometers. In this fitting procedure, we set the Gauss width of the Voigt function to be 3.7 eV based on the estimates of the experimental beam broadening. As summarized in Table I, the largest contribution to the resonance width was by the longitudinal momentum spread of the beam, which was estimated to be $\Delta p/p = 7 \times 10^{-4}$ from the SIS. The second largest contribution was from the energy loss of the incident beam in the target crystal, i.e., the change in beam energy during penetration. Other contributions resulting from the beam divergence as well as angular and energy straggling in the target are also listed in the table, although they had only minor contributions compared with those described above. The inhomogeneous Stark broadening induced by the static planar field in the channel [24] is negligibly small due to the large energy separation between the $n = 2$ levels in the U^{89+} ion. According to these estimates, the Lorentz width of the Voigt profile is obtained to be 1.3 eV. Because the natural width due to the spontaneous emission is as small as ~0.1 eV [30], the collisional decoherence in the target is considered to be essential for this Lorentz width. Thus, the decoherence rate of the interaction is revealed to be 1×10^{15} s^{-1}, which corresponds to a traveling distance of 0.2 μm in the crystal. It should be noted that the inelastic collision rate estimated from the excitation and ionization cross sections [27] is of the order of 10^{13} s^{-1}. This suggests that the decoherence is predominantly caused by elastic collision processes.

The above analysis manifests that the spectroscopic resolution of this method can be further improved by enhancing the quality of the ion beam. In addition, the absolute transition energy can be precisely determined, if the uncertainty in beam energy is reduced. A breakthrough approach satisfying both these requirements is to use an ion storage ring. Using the

electron cooler in the experimental storage ring (ESR) at GSI will reduce the momentum spread $\Delta p/p$ to the order of 10^{-5}, which is one order of magnitude smaller than that achieved with the SIS. The absolute energy of the ion beam can be calibrated with high precision from the voltage of the electron cooler. Moreover, use of a thinner target will reduce the energy loss of projectile ions in the target. In particular, for a 0.7-μm-thick crystal, which was already used in the recent RCE experiments at HIMAC, the energy loss in the crystal will be reduced to one tenth. These improvements would bring our method to a comparable level with the most accurate results from crystal spectrometers [31], allowing for the determination of, for example, the two-loop QED contribution to the $2s$ Lamb shift in high-Z ions. It should be noted that reducing the crystal thickness will increase the resonance width coming from the uncertainty principle and the Fourier width. However, if we use the 0.7-μm-thick crystal, the width coming from the uncertainty principle is 50 meV, which is still smaller than other factors. The Fourier width will matter if the target is thinner than the coherence length of the interaction, which was estimated to be $\sim$0.2 μm from the observed resonance width.

In summary, we have successfully applied the RCE technique to highly charged uranium ions, proving its versatility for resonant fluorescence spectroscopy of high-Z ions in the x-ray domain. The excitation efficiency was proven to be $\sim$80%, which is high enough to examine a small amount of ions from accelerators as a universal tool for atomic and nuclear physics. The observed resonance width was 4.4 eV at a transition energy of $4460.9 \pm 0.1 \pm 2.2$ eV, which was found to be mostly limited by broadening of the ion-beam velocity. It was also shown that the improvement of the ion-beam quality by using an electron cooler in the storage ring and an extremely thin target crystal will enable resonance fluorescence spectroscopy with high resolution and accuracy. A test experiment with a cooled U^{89+} beam extracted from the ESR was recently successfully performed. An upgrade of the beam line for better transportation of the cold beam is in the planning phase.

This study was supported in part by a Grants-in-Aid for Scientific Research (No. 19104010) from the Japan Society for the Promotion of Science (JSPS). Y.N. acknowledges support from JSPS (No. 22840050 and No. 23740311).

[1] C. G. Parthey, A. Matveev, J. Alnis, B. Bernhardt, A. Beyer, R. Holzwarth, A. Maistrou, R. Pohl, K. Predehl, T. Udem *et al.*, Phys. Rev. Lett. **107**, 203001 (2011).

[2] Y. Zou and R. Hutton, *Handbook for Highly Charged Ion Spectroscopic Research* (Taylor & Francis, New York, 2011), Chap. 1.

[3] J. Eichler and T. Stöhlker, Phys. Rep. **439**, 1 (2007).

[4] S. W. Epp, J. R. C. López-Urrutia, G. Brenner, V. Mäckel, P. H. Mokler, R. Treusch, M. Kuhlmann, M. V. Yurkov, J. Feldhaus, J. R. Schneider *et al.*, Phys. Rev. Lett. **98**, 183001 (2007).

[5] V. V. Okorokov, JETP Lett. **2**, 111 (1965).

[6] S. Datz, C. D. Moak, O. H. Crawford, H. F. Krause, P. D. Miller, P. F. Dittner, J. G. del Campo, J. A. Biggerstaff, H. Knudsen, and P. Hvelpumd, Nucl. Instrum. Methods **170**, 15 (1980).

[7] F. Fujimoto, K. Komaki, A. Ootuka, E. Vilalta, Y. Iwata, Y. Hirao, T. Hasegawa, M. Sekiguchi, A. Mizobuchi, T. Hattori *et al.*, Nucl. Instrum. Methods B **33**, 354 (1988).

[8] S. Datz, P. F. Dittner, H. F. Krause, C. R. Vane, O. H. Crawford, J. S. Forster, G. S. Ball, W. G. Davies, and J. S. Geiger, Nucl. Instrum. Methods B **100**, 272 (1995).

[9] J. S. Forster, G. C. Ball, W. G. Davies, J. S. Geiger, J. U. Andersen, J. A. Davies, H. Geissel, and F. Nickel, Nucl. Instrum. Methods B **107**, 27 (1996).

[10] T. Azuma, T. Ito, K. Komaki, Y. Yamazaki, M. Sano, M. Torikoshi, A. Kitagawa, E. Takada, and T. Murakami, Phys. Rev. Lett. **83**, 528 (1999).

[11] H. Kudo, M. Nagata, H. Wakamatsu, and S. Tomita, Nucl. Instrum. Methods B **229**, 227 (2005).

[12] T. Azuma, Y. Takabayashi, C. Kondo, T. Muranaka, K. Komaki, Y. Yamazaki, E. Takada, and T. Murakami, Phys. Rev. Lett. **97**, 145502 (2006).

[13] S. Datz, C. D. Moak, O. H. Crawford, H. F. Krause, P. F. Dittner, J. Gomez del Campo, J. A. Biggerstaff, P. D. Miller, P. Hvelplund, and H. Knudsen, Phys. Rev. Lett. **40**, 843 (1978).

[14] Y. Nakai, Y. Nakano, T. Azuma, A. Hatakeyama, C. Kondo, K. Komaki, Y. Yamazaki, E. Takada, and T. Murakami, Phys. Rev. Lett. **101**, 113201 (2008).

[15] Y. Nakano, C. Kondo, A. Hatakeyama, Y. Nakai, T. Azuma, K. Komaki, Y. Yamazaki, E. Takada, and T. Murakami, Phys. Rev. Lett. **102**, 085502 (2009).

[16] Y. Nakano, S. Suda, A. Hatakeyama, Y. Nakai, K. Komaki, E. Takada, T. Murakami, and T. Azuma, Phys. Rev. A **85**, 020701(R) (2012).

[17] T. Aumann, K. Langanke, K. Peters, and T. Stöhlker, EPJ Web Conf. **3**, 01006 (2010).

[18] V. V. Balashov, A. A. Sokolik, and A. V. Stysin, JETP **107**, 133 (2008).

[19] N. Claytor, B. Feinberg, H. Gould, C. E. Bemis, J. Gomez del Campo, C. A. Ludemann, and C. R. Vane, Phys. Rev. Lett. **61**, 2081 (1988).

[20] D. Dauvergne, C. Scheidenberger, A. L'Hoir, J. U. Andersen, S. Andriamonje, C. Böckstiegel, M. Chevallier, C. Cohen, N. Cue, S. Czajkowski *et al.*, Phys. Rev. A **59**, 2813 (1999).

[21] C. Ray, A. Bräuning-Demian, H. Bräuning, M. Chevallier, C. Cohen, D. Dauvergne, A. L'Hoir, C. Kozhuharov, D. Liesen, P. H. Mokler *et al.*, Phys. Rev. B **84**, 024119 (2011).

[22] P. Beiersdorfer, D. Knapp, R. E. Marrs, S. R. Elliott, and M. H. Chen, Phys. Rev. Lett. **71**, 3939 (1993).

[23] P. Beiersdorfer, Nucl. Instrum. Methods B **99**, 114 (1995).

[24] K. Komaki, T. Azuma, T. Ito, Y. Takabayashi, Y. Yamazaki, M. Sano, M. Torikoshi, A. Kitagawa, E. Takada, and T. Murakami, Nucl. Instrum. Methods B **146**, 19 (1998).

[25] Y. Nakai, T. Ikeda, Y. Kanai, T. Kambara, N. Fukunishi, T. Azuma, K. Komaki, Y. Takabayashi, and Y. Yamazaki, Nucl. Instrum. Methods B **205**, 784 (2003).

[26] Y. Nakano, Y. Takano, T. Shindo, T. Ikeda, Y. Kanai, S. Suda, T. Azuma, H. Bräuning, A. Bräuning-Demian, T. Stöhlker *et al.*, Phys. Scr. T **144**, 014010 (2011).

[27] C. Scheidenberger, T. Stöhlker, W. E. Meyerhof, H. Geissel, P. H. Mokler, and B. Blank, Nucl. Instrum. Methods B **142**, 441 (1998).

[28] T. Ito, T. Azuma, K. Komaki, Y. Yamazaki, M. Sano, M. Torikoshi, A. Kitagawa, E. Takada, and T. Murakami, Nucl. Instrum. Methods B **135**, 132 (1998).

[29] ATIMA, http://www-linux.gsi.de/∼weick/atima/.

[30] C. E. Theodosiou, L. J. Curtis, and M. El-Mekki, Phys. Rev. A **44**, 7144 (1991).

[31] P. Beiersdorfer, H. Chen, D. B. Thorn, and E. Träbert, Phys. Rev. Lett. **95**, 233003 (2005).